

# Fabrication and characterization of $(\text{Pb}(\text{Mg}_{1/3}\text{Nb}_{2/3})\text{O}_3, \text{Pb}(\text{Yb}_{1/2}\text{Nb}_{1/2})\text{O}_3, \text{PbTiO}_3)$ ternary system ceramics

Erdem Akça\*, Cihangir Duran

Department of Materials Science and Engineering, Gebze Institute of Technology, P.K. 141, 41400, Gebze, Kocaeli, Turkey

Received 9 November 2010; received in revised form 12 February 2011; accepted 1 March 2011

Available online 8 April 2011

## Abstract

New ternary compositions in the  $\text{Pb}(\text{Mg}_{1/3}\text{Nb}_{2/3})\text{O}_3$ – $\text{Pb}(\text{Yb}_{1/2}\text{Nb}_{1/2})\text{O}_3$ – $\text{PbTiO}_3$  (PMN–PYbN–PT) system were prepared using 0.5 $\text{Pb}(\text{Yb}_{1/2}\text{Nb}_{1/2})\text{O}_3$ –0.5 $\text{PbTiO}_3$  (PYbNT) and  $(1-x)\text{Pb}(\text{Mg}_{1/3}\text{Nb}_{2/3})\text{O}_3$ – $x\text{PbTiO}_3$  ( $x = 0.26$ ; PMNT26 or  $x = 0.325$ ; PMNT32.5) powders synthesized via the columbite method. Dense ( $\geq 96\%$  of theoretical density) ceramics with PMN/PYbN mole ratios of 25/75 (R-25), 50/50 (R-50) and 75/25 (R-75T and R-75R) were fabricated by reactive sintering at 1000 °C for 4 h. Therefore, incorporation of PYbNT to PMNT successfully decreased sintering temperature of PMNT from 1200 °C–1250 °C to 1000 °C. Samples with higher density and perovskite ratio together with lower weight loss possessed higher dielectric and piezoelectric values in each composition. The R-75 samples had remanent polarization ( $P_r$ ) values of 34–36  $\mu\text{C}/\text{cm}^2$  and piezoelectric charge coefficient ( $d_{33}$ ) of 560 pC/N. The sharp phase transition PMNT as a function of temperature became broader or more diffuse with increasing PYbNT content. However, PYbNT addition to PMNT increased Curie temperature ( $T_c$ ) from 183 °C (for PMNT32.5) to 220–242 °C (for R-75T and R-75R) to 336 °C (for R-25). Therefore, these ternary compositions can be tailored for various high temperature applications due to the relatively higher  $T_c$  with enhanced piezoelectric and dielectric properties as compared to PMNT.

© 2011 Elsevier Ltd and Techna Group S.r.l. All rights reserved.

**Keywords:** A. Sintering; C. Ferroelectric properties; C. Dielectric properties; D. Perovskites

## 1. Introduction

Lead-based relaxor ceramics with a general formula  $\text{Pb}(\text{B}_1\text{B}_2)\text{O}_3$  have excellent dielectric and piezoelectric properties [1–5]. Relaxor  $\text{Pb}(\text{Mg}_{1/3}\text{Nb}_{2/3})\text{O}_3$  (PMN) ferroelectric (FE) possesses good voltage stability, superior electrostrictive effects, low sintering temperature and a dielectric response. However, its Curie temperature ( $T_c$ ) is approximately  $-15^\circ\text{C}$ , which restricts many device applications [6–10]. The  $T_c$  of PMN can be increased by adding a normal FE  $\text{PbTiO}_3$  (PT) with a higher  $T_c$  ( $\sim 490^\circ\text{C}$ ) [6,7]. The  $T_c$  is shifted to higher temperatures due to the formation of a solid solution between PT and PMN.  $(1-x)\text{PMN}$ – $x\text{PT}$  system, which displays good piezoelectric and pyroelectric properties near a morphotropic phase boundary (MPB) (between 0.3 and 0.35 mol% PT) [8]. Accordingly, dielectric and electromechanical properties are also changed due to the formation of a MPB [8,11].

Conventional and reactive sintering methods have been applied to densify PMN–PT ceramics [12,13]. Reactive sintering

is a process in which phase formation and densification are both achieved in the same heat treatment. However, the two steps can occur concurrently or in sequence, depending on processing and starting materials [14]. 0.68PMN–0.32PT ceramics with 4 wt% excess PbO were reactively sintered at 1250 °C via the columbite method [15]. These ceramics had a remnant polarization ( $P_r$ )  $\sim 21 \mu\text{C}/\text{cm}^2$ , a coercive field ( $E_c$ )  $\sim 8.8 \text{ kV}/\text{cm}$ ,  $T_c \sim 190^\circ\text{C}$ , and a piezoelectric charge coefficient ( $d_{33}$ )  $\sim 325 \text{ pC}/\text{N}$  [15]. The  $d_{33}$  was found to be 590 pC/N for the same composition that consisted of 0.5 wt% excess PbO [16]. Whereas, 0.68PMN–0.32PT ceramics fabricated at 1230 °C via one-step calcination without excess PbO possess  $P_r \sim 26.2 \mu\text{C}/\text{cm}^2$ ,  $E_c \sim 4.1 \text{ kV}/\text{cm}$ ,  $T_c \sim 138^\circ\text{C}$ , and  $d_{33} \sim 458 \text{ pC}/\text{N}$  [17].

The dielectric and piezoelectric properties are enhanced near the MPB compositions because of large number of polarization directions available. High dielectric and piezoelectric properties associated with low  $T_c$  come at the expense of more temperature-dependent properties and low depoling temperatures. Thus, ceramic compositions near MPB with high  $T_c$  are desired [18]. Although PMN–PT ceramics have good FE properties, their  $T_c$ 's are quite low which restricts the working range of the devices based on these materials. Our recent work

\* Corresponding author. Tel.: +90 262 605 1733; fax: +90 262 653 0675.

E-mail address: [erdemig@ gmail.com](mailto:erdemig@ gmail.com) (E. Akça).

showed that the addition of a high  $T_c$  ceramic (e.g.,  $0.5\text{Pb}(\text{Yb}_{1/2}\text{Nb}_{1/2})\text{O}_3$ – $0.5\text{PbTiO}_3$ , hereafter referred to as PYbNT) increased the  $T_c$  of the PMN–PT composition without degrading the electrical properties [19].  $(1-x)\text{PYbN}$ – $x\text{PT}$  solid solution has a MPB composition at  $x = 0.5$  with a  $T_c \sim 360^\circ\text{C}$  [18,20]. In addition, PYbNT ceramics reactively sintered at temperatures as low as  $950^\circ\text{C}$  using 3 wt% excess PbO were reported to have enhanced dielectric and piezoelectric properties such as  $P_r \sim 36 \mu\text{C}/\text{cm}^2$ ,  $E_c \sim 22 \text{ kV}/\text{cm}$  and  $d_{33} \sim 508 \text{ pC}/\text{N}$  together with a high  $T_c \sim 371^\circ\text{C}$  [20].

The objective of this study is to formulate ceramic compositions in ternary PMN–PYbN–PT system to achieve enhanced dielectric and piezoelectric properties. PMN/PYbN mole ratio at 25/75, 50/50 and 75/25 will be primarily discussed based on our previous 50/50 mole ratio study [19]. With the addition of PYbNT to PMNT, the  $T_c$  of the latter can be increased and the sintering temperature of the ternary system can be decreased. Ultimately, the objective is to produce ternary compositions with enhanced properties and to provide temperature stability for higher temperature device applications. Densification, phase formation as a function of sintering temperature between  $950^\circ\text{C}$  and  $1200^\circ\text{C}$  and dielectric and piezoelectric properties are also reported.

## 2. Experimental Procedure

$(\text{MgCO}_3)_4 \cdot \text{Mg}(\text{OH})_2 \cdot 5\text{H}_2\text{O}$  (Sigma-Aldrich Chemie GmbH, Germany),  $\text{Nb}_2\text{O}_5$  (Alfa Aesar GmbH & Co. KG, Germany),  $(\text{PbCO}_3)_2 \cdot \text{Pb}(\text{OH})_2$  (Alfa Aesar),  $\text{TiO}_2$  (Evonik Degussa Industries AG, Germany) and  $\text{Yb}_2\text{O}_3$  (Alfa Aesar) were used as starting materials. The steps involved in the synthesis of powders and final compositions are summarized in Table 1. All powders were mixed in a Nalgene<sup>TM</sup> (Nalgene Labware, Denmark) bottle by ball milling using  $\text{ZrO}_2$  media in isopropyl alcohol and then dried on a hot plate at  $50^\circ\text{C}$  with continuous stirring. Calcined powders were again ball milled for 24 h to reduce particle size down to  $\leq 1 \mu\text{m}$  range.

The appropriate amounts of PMNT32.5 (or PMNT26) and PYbNT were milled together to prepare ternary PMN–PYbN–PT compositions based on Table 1. The end composition powders, PMNT26, PMNT32.5 and PYbNT, were synthesized

by the columbite method [21]. Samples were first hand-pressed (12 mm diameter) with no binder addition and then cold isostatically pressed at 80 MPa for 3 min. The samples were sintered in air at  $950$ – $1200^\circ\text{C}$  for 4 h with a heating rate of  $5^\circ\text{C}/\text{min}$  and cooling rate of  $10^\circ\text{C}/\text{min}$ . During sintering, the samples were contained within a double-crucible setup with sacrificial  $\text{PbO}/\text{ZrO}_2$  powders placed between the walls of the two  $\text{Al}_2\text{O}_3$  crucibles to control PbO atmosphere inside.

Density of sintered samples was measured by the Archimedes' technique. Weight loss was calculated by comparing the weight of the samples before and after sintering. The phase formation for both powders and sintered ceramics were checked using an X-ray diffractometer (Bruker D8 Advanced, Bruker AXS GmbH, Germany). The amount of perovskite phase was calculated based on the XRD patterns by comparing the strongest intensity peaks of the perovskite and pyrochlore phases [21]. The surfaces of samples were polished using 1200-grit SiC paper before electrical measurements. Before the dielectric polarization and piezoelectric measurements, the samples were electroded by silver paste and then baked in air at  $600^\circ\text{C}$  for 30 min. The variation of dielectric constant and loss tangent as a function of frequency from room temperature up to  $450^\circ\text{C}$  were measured using an inductance-capacitance-resistance (LCR) meter (Hioki, E.E. Co. Japan). The polarization and coercive field were estimated from the polarization–electric field (P–E) hysteresis loops recorded at room temperature and at 1.3 Hz using a FE testing unit Precision LC (Radiant Inc., USA). Poling was performed in silicone oil at  $120^\circ\text{C}$  for 15 min at a field of 20–30 kV/cm. The piezoelectric charge coefficient,  $d_{33}$ , was measured 24 h after poling using a Berlincourt  $d_{33}$  meter (American Piezo Ceramics Inc., APC International Ltd., USA).

## 3. Results and discussion

### 3.1. Phase formation and densification

XRD patterns in Fig. 1 show the phase evolution of the R-75T samples as a function of sintering temperature between  $950^\circ\text{C}$  and  $1200^\circ\text{C}$  for 4 h. Single perovskite phase was maintained up to  $1200^\circ\text{C}$ ; however, a non-perovskite pyrochlore phase (marked as \*) was observed in ceramics sintered at

Table 1  
Sample designation, starting and final matrix compositions.

Designation	Starting compositions	Final compositions	Calcination conditions
MN	$(\text{MgCO}_3)_4 \cdot \text{Mg}(\text{OH})_2 \cdot 5\text{H}_2\text{O} + \text{Nb}_2\text{O}_5$	$\text{MgNb}_2\text{O}_6$	$1150^\circ\text{C}$ –4h
YbN	$\text{Yb}_2\text{O}_3 + \text{Nb}_2\text{O}_5$	$\text{YbNbO}_4$	$1200^\circ\text{C}$ –4h
PT	$(\text{PbCO}_3)_2 \cdot \text{Pb}(\text{OH})_2 + \text{TiO}_2$	$\text{PbTiO}_3$	$800^\circ\text{C}$ –2h
PYbN	$(\text{PbCO}_3)_2 \cdot \text{Pb}(\text{OH})_2 + \text{YbN}$	$\text{Pb}(\text{Yb}_{1/2}\text{Nb}_{1/2})\text{O}_3$	$900^\circ\text{C}$ –2h
PYbNT	PYbN + PT + 3 wt% PbO	$0.5\text{Pb}(\text{Yb}_{1/2}\text{Nb}_{1/2})\text{O}_3$ – $0.5\text{PbTiO}_3$	$875^\circ\text{C}$ –4h
PMNT32.5	$(\text{PbCO}_3)_2 \cdot \text{Pb}(\text{OH})_2 + \text{MN} + \text{TiO}_2$	$0.675\text{Pb}(\text{Mg}_{1/3}\text{Nb}_{2/3})\text{O}_3$ – $0.325\text{PbTiO}_3$	$875^\circ\text{C}$ –4h
PMNT26	$(\text{PbCO}_3)_2 \cdot \text{Pb}(\text{OH})_2 + \text{MN} + \text{TiO}_2$	$0.74\text{Pb}(\text{Mg}_{1/3}\text{Nb}_{2/3})\text{O}_3$ – $0.26\text{PbTiO}_3$	$875^\circ\text{C}$ –4h
R-25 *	PMNT32.5 + PYbNT	$0.535[0.25\text{PMN}-0.75\text{PYbN}]-0.465\text{PT}$	–
R-50 #	PMNT32.5 + PYbNT	$0.575[0.5\text{PMN}-0.5\text{PYbN}]-0.425\text{PT}$	–
R-75T †	PMNT32.5 + PYbNT	$0.62[0.75\text{PMN}-0.25\text{PYbN}]-0.38\text{PT}$	–
R-75R †	PMNT26 + PYbNT	$0.66[0.75\text{PMN}-0.25\text{PYbN}]-0.34\text{PT}$	–

Excess PbO was added in the form of  $(\text{PbCO}_3)_2 \cdot \text{Pb}(\text{OH})_2$ .

\*, †, #: Total excess PbO (\*: 1.5 wt%, #: 1.1 wt%, †: 0.7 wt%).

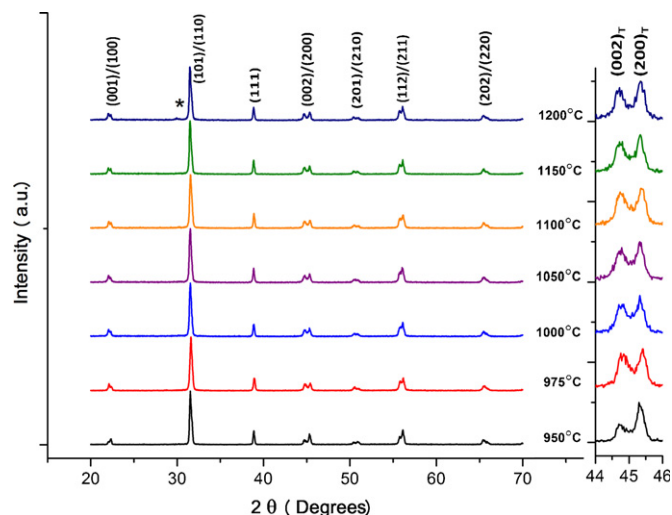


Fig. 1. XRD patterns of the R-75T samples as a function of sintering temperature. The splitting in {200} peak near  $2\theta \sim 45^\circ$  is given as inset. \* refers to pyrochlore phase.

1200 °C for 4 h. The reflections from tetragonal phase (as shown in inset in Fig. 1) are clearly seen from splitting in {200} peaks near  $2\theta \sim 45^\circ$ .

Fig. 2 compares the XRD patterns of the PMN-PYbN-PT based ceramics sintered at 1000 °C for 4 h and splitting in {200} peaks near  $2\theta \sim 45^\circ$ . Since the main peaks of the R-25, R-50, R-75R and R-75T samples (sintered at 1000 °C for 4 h) are located at  $2\theta \sim 31.16^\circ$ ,  $31.34^\circ$ ,  $31.4^\circ$  and  $31.47^\circ$  respectively, which are between the main peaks of PMNT32.5 ( $2\theta \sim 31.51^\circ$ ) or PMNT26 ( $2\theta \sim 31.48^\circ$ ) and PYbNT ( $2\theta \sim 31.02^\circ$ ) end compositions. The final ternary compositions are said to be solid solutions between PMNT32.5 or PMNT26 and PYbNT [19]. Also, the R-50, R-75T and R-75R ceramics sintered 1000 °C for 4 h consisted of single phase perovskite; however, the R-25 ceramic contained some pyrochlore phase. In addition, the splitting in {200} peaks near  $2\theta \sim 45^\circ$  indicates that the R-75R ceramic have completely rhombohedral phase, the R-50 and R-75T ceramics possess tetragonal phase, and the R-25 ceramic has a coexistence of both tetragonal and rhombohedral phases. In a previous work [22], the MPB's of PMN-PYbN-PT compositions were determined to be in

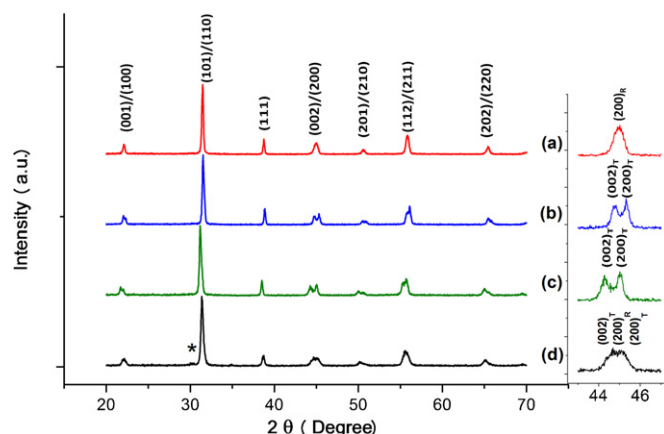


Fig. 2. XRD patterns of the PMN-PYbN-PT ceramics sintered at 1000 °C for 4 h: (a) R-75R, (b) R-75T, (c) R-50 and (d) R-25. The splitting in {200} peak near  $2\theta \sim 45^\circ$  is given as inset.

between 32–35 mol% PT for PMN/PYbN (75/25), 37–40 mol% PT for PMN/PYbN (50/50) and 44–47 mol% PT for PMN/PYbN (25/75). In this work, since the R-25 ceramics have  $\sim 46.5$  mol% PT, which is very close to MPB, the tetragonal phase coexists with the rhombohedral phase.

The theoretical density of the sintered ceramics was determined based on the respective theoretical densities of PMNT32.5 (or PMNT26) and PYbNT ceramics and calculated to be as 8.30 g/cm<sup>3</sup>, 8.13 g/cm<sup>3</sup>, 8.24 g/cm<sup>3</sup> and 8.25 g/cm<sup>3</sup> for the R-25, R-50, R-75T and R-75R, respectively. Table 2 depicts the variation of the % relative density ( $\rho$ ), % perovskite ratio (PR) and % weight loss (WL) of PMN-PYbN-PT ceramics as a function of sintering temperature. The weight loss was found after the initially-added excess PbO was subtracted. Note that different excess PbO amounts given in Table 1 is due to the fact that only PYbNT has 3 wt% initial excess PbO; therefore, excess PbO amount in the ternary compositions varied depending on the PMN/PYbN ratios.

The R-25 ceramics with full perovskite phase were never fabricated in this study. Maximum perovskite ratio was calculated to be 97% at 1000 °C; however, it decreased down to 65.5% at 1200 °C. Densification of the R-25 ceramics exhibited a similar trend as perovskite ratio. Maximum relative density was 96.7% at 1050 °C but it decreased down to 91.7%

Table 2

The % relative density ( $\rho$ ), % perovskite ratio (PR) calculated from XRD patterns and % weight loss (WL) in the samples as a function of sintering temperature for 4 h (– denotes weight loss after sintering).

Samples	Properties	950 °C	975 °C	1000 °C	1050 °C	1100 °C	1150 °C	1200 °C
R-25	$\rho$	86.8	90	96	96.7	96.5	94	91.7
	WL	–0.68	–0.84	–2.76	–5.2	–9.39	–13.57	–16.18
	PR	94	96	97	89.5	82.1	74.2	65.5
R-50	$\rho$	98.5	98.8	98.4	98.4	97.4	96.1	94.1
	WL	–1.35	–1.45	–2.27	–3.05	–4.16	–6.66	–10.41
	PR	100	100	100	93.6	92.3	90.5	74.6
R-75T	$\rho$	96	96.5	95	95.3	95.7	96.1	94.8
	WL	–2.03	–2.33	–1.98	–2.02	–2.1	–2.25	–2.71
	PR	100	100	100	100	100	100	94
R-75R	$\rho$	96.9	97.2	96.9	96.9	96.5	96.2	96.1
	WL	–0.33	–0.26	–0.18	–0.28	–0.43	–0.52	–1.34
	PR	100	100	100	100	100	100	95.8

at 1200 °C. On the other hand, lower densification was observed for the R-25 ceramics at temperatures less than 1000 °C. Similar behaviors were also observed for the R-50 and R-75 compositions with the exception that higher density and perovskite ratio were retained up to higher temperatures. For example, full perovskite ratio was retained up to 1000 °C for the R-50 and 1150 °C for the R-75 samples. Weight loss was facilitated remarkably towards higher temperatures.

The tolerance factor ( $t$ ) and electronegativity difference ( $\Delta\chi$ ) were reported as the most important requirements for the stabilization of perovskite structure [23]. When  $t$  is close to 1 and  $\Delta\chi$  is high as much as possible simultaneously, better formation and higher stabilization of the perovskite structure can be obtained for  $A(B_1B_2)O_3$  type compositions. It was reported that  $t=0.99$  and  $\Delta\chi=1.85$  for PMN,  $t=1.01$  and  $\Delta\chi=1.8$  for PT [23],  $t=0.95$  and  $\Delta\chi=2$  for PYbN [24]. Especially, the mean radius of the B-site ions was stated as the most important factor limiting the perovskite structure. For the systems with larger B-site cations, the A-O and B-O bondings are not strong enough to construct a perovskite structure including an octahedral of B-site cations surrounded by oxygens. The ionic radii of B-site ions  $Yb^{3+}$ ,  $Nb^{5+}$ ,  $Mg^{2+}$  and  $Ti^{4+}$  in PMN-PYbN-PT system are 1.008 Å, 0.78 Å, 0.86 Å and 0.745 Å, respectively [25]. Since increasing PYbN amount in PMN-PYbN-PT ternary systems (in other words, decreasing PMN/PYbN mole ratio) causes increasing the mean ratio of B-site ions due to the presence of  $Yb^{3+}$  ions with higher ionic radii,  $t$  value of ternary system decreases. Although  $\Delta\chi$  values of PMN-PYbN-PT ceramics ( $\sim 1.87$ ) are close to each other, the calculated tolerance factor values are sequenced as  $t_{R-25}$  ( $0.986$ ) <  $t_{R-50}$  ( $0.989$ ) <  $t_{R-75R}$  ( $0.992$ ) <  $t_{R-75T}$  ( $0.994$ ). Therefore, higher perovskite ratios were observed in PMN-PYbN-PT based ceramics with higher  $t$  values (R-75T and R-75R) because higher PMN/PYbN mole ratios resulted in increasing  $t$  due to decreasing the mean radius of B-site ions (see Table 2). Lower  $t$  should be taken into account to understand why full perovskite structures could not be stabilized especially for the R-25 samples.

Table 2 reveals in general that as weight loss increases with increasing sintering temperature, both perovskite ratio and densification decrease. PbO evaporation with temperature induces a non-perovskite lead-deficient pyrochlore phase formation [26–28], which negatively affects both perovskite stability and densification. Although sintering was carried out in a double crucible setup, initially-added excess PbO (See Table 1) and atmosphere powder could not compensate PbO evaporation at higher temperatures. Pyrochlore formation may be attributed to the degradation of PYbN at higher sintering temperatures [20,24]. However, both densification degree and perovskite ratio were shown to decrease severely after sintering above 1000 °C due to non-perovskite phase formation. Therefore, PYbNT addition does decrease sintering temperature in PMN-PYbN-PT ternary ceramics, as also shown in Table 2. Dense samples (e.g., theoretical density  $\geq 96\%$ ) together with high perovskite ratio in each composition were obtained at around 1000 °C, which is much less than the sintering temperature of PMNT ceramics (i.e., 1200 °C–1250 °C) [15].

### 3.2. Dielectric and piezoelectric properties

Higher densification (i.e., > 95%) and 100% perovskite formation are very critical processing parameters to be aimed in lead-based ferroelectric ceramics because they are closely related with ferroelectric properties [20,29,30]. Samples follow a similar trend with the processing parameters (e.g., density, perovskite ratio and weight loss as shown in Table 2), therefore, samples with higher density and perovskite ratio together with lower weight loss possess higher dielectric values in each composition. Room temperature dielectric constants ( $K$ ) and dielectric losses ( $\tan\delta$ ) of poled ternary compositions (measured at 1 kHz) are compared as a function of sintering temperature in Fig. 3. Samples sintered at around 1000 °C for 4 h reached their respective maximum values. The dielectric constants and losses decreased after sintering temperatures > 1000 °C, (particularly for R-50 and R-25) because existence of pyrochlore phase together with lower density unfavorably affected the dielectric properties [19]. The pyrochlore phase with a low  $K \sim 200$  (or PbO with  $K \sim 26$  [31]) was reported to have a harmful effect on the dielectric constant of PMNT and PYbNT ceramics in literature [20,27]. The R-25 ceramics possessed the lowest dielectric constants among the samples in the studied temperature regime because full perovskite ratio was never obtained. As PMN/PYbN mole ratio increases, the  $K$  of the ternary compositions enhances. For example, the  $K$  values obtained are found to be 1560, 2380, 2720 and 3450 for the R-25, R50, R-75R and R-75T ceramics sintered at 1000 °C, respectively. This is consistent with the respective  $K$  values of PMNT and PYbNT; that is,  $K = 2500$ – $3000$  [19] and  $K = 1920$  [20], respectively. In addition, 0.68PMN-0.32PT (PMNT32) ceramics near MPB was reported to be as the highest dielectric constant for PMNT based ceramics [15]. Therefore, if samples with the same PMN/PYbN mole ratio (75/25) are compared, it

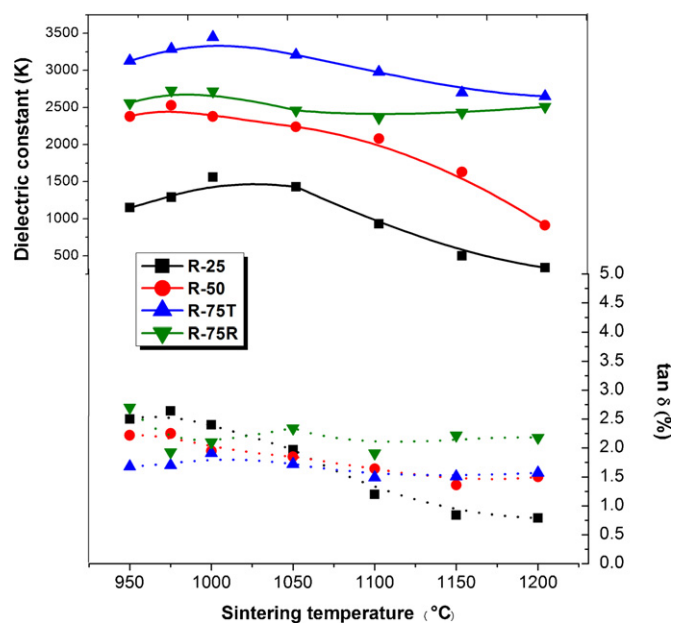


Fig. 3. Dielectric constant ( $K$ ) and loss ( $\tan\delta$ ) of poled samples (at 1 kHz and room temperature) as a function of sintering temperature.



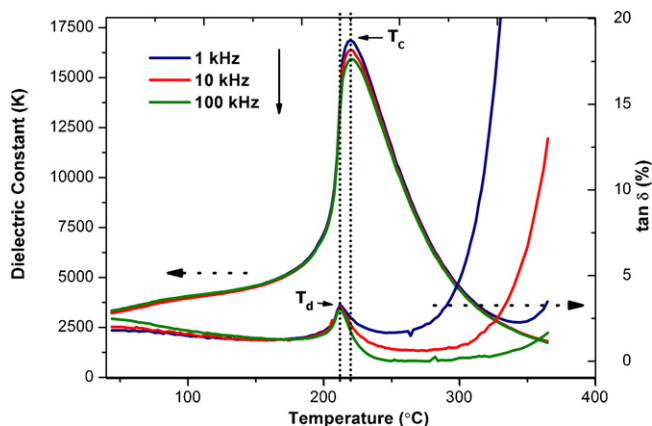


Fig. 4. Dielectric behavior of poled R-75T ceramic sintered at 1000 °C for 4 h as a function increasing temperature and frequency.

can be inferred that the R-75T ceramics including PMNT32.5, which is very close to MPB region, have higher  $K$  than R-75R ceramics formed from PMNT26. Besides, the  $\tan\delta$  values (approximately 2%) were very close to other samples sintered at 1000 °C for 4 h. However, the  $\tan\delta$  usually declined with increasing sintering temperature especially after 1000 °C for the R-25 ceramics, which can also be related with the pyrochlore formation and lower densification.

Fig. 4 shows temperature and frequency dependence of dielectric constant and loss for poled R-75T sample during heating. The sample has a sharp transition from ferroelectric to paraelectric phase at a Curie temperature ( $T_c$ ) of  $\sim 220$  °C. The maximum dielectric constant ( $K_{\max}$ ) is found to be 16900 near  $T_c$ .  $K_{\max}$  values correspond to the same temperature (e.g.,  $T_c$  in this case) at various frequencies indicate that the R-75T sample has a normal ferroelectric behavior without any frequency dispersion. In addition, dielectric loss behavior indicates that depolarization temperature ( $T_d$ ) is different from the  $T_c$  (see dotted vertical lines in Fig. 4). The  $T_d$  is also corresponds to a specific temperature where pyroelectric current maximum occurs. The difference between  $T_c$  and  $T_d$  were calculated to be 3 °C, 2 °C, 8 °C and 24 °C for the PMNT32.5, R-75T, R-50 and R-75R ceramics, respectively. The temperature of dielectric loss maxima was not observed for the R-25 sample because of poor densification and pyrochlore formation. In fact, dielectric loss vs. temperature plot (not shown here) for the R-25 sample indicated that loss increases sharply at around 225 °C, which is well below the  $T_c = 336$  °C indicating the onset of electrical conduction with temperature due to conductive grain boundary phases [20]. It has been documented in literature that second phases such as unreacted PbO and PbO-rich phases segregate in the grain boundaries, making grain boundaries conductive [27,28,32]. Measurement of dielectric properties using poled samples as a function of temperature is important to detect phase transitions below  $T_c$  if the ceramic composition is located near a MPB. Fig. 4 indicates that there is a shallow hump at around 100 °C, which indicates rhombohedral (R) to tetragonal (T) phase transition.

Fig. 5 compares temperature and frequency dependence of dielectric constant and loss for poled ternary compositions

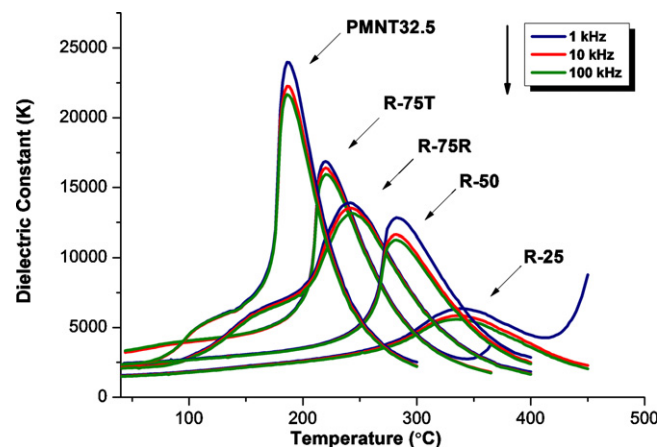


Fig. 5. Dielectric constant of all PMN-PYbN-PT based ceramics sintered at 1000 °C for 4 h and PMNT-32.5 sintered at 1200 °C for 6 h.

sintered at 1000 °C for 4 h and PMNT32.5 sintered at 1200 °C for 6 h. The  $T_c$  values were determined to be 183 °C, 220 °C, 242 °C, 282 °C and 336 °C for the PMNT32.5, R-75T, R-75R, R-50 and R-25, respectively. Because PYbNT has a higher  $T_c$  ( $\sim 371$  °C) [20], the  $T_c$  values of ternary compositions change accordingly.  $K_{\max}$  values decreases with increasing PYbNT content. In addition, sharp phase transition of PMNT32.5 becomes broader or more diffuse with increasing PYbNT content.

Diffuse phase transition (DPT) and degree of DPT can be attributed to B-site cations and their ionic radii in the perovskite structure. In the previous section, perovskite stability was correlated with the tolerance factor ( $t$ ). More PYbN amount in PMN-PYbN-PT ternary systems (in other words, decreasing PMN/PYbN mole ratio) increases the mean radius of B-site ions due to the presence of bigger Yb<sup>3+</sup> cations, which decreases  $t$  but, at the same time, increases DPT due possibly to nonhomogenous disorder in perovskite structure [27,33–36]. B-site compositional fluctuations on a nanometer scale gives rise to DPT for Pb(B'<sub>1</sub>B''<sub>2</sub>)O<sub>3</sub>-based perovskites. For example, A-site Pb<sup>2+</sup> ion is not responsible for compositional fluctuations for PMN [27]. On the other hand, the addition of PbZrO<sub>3</sub> (PZ) to PYbN weakens the order of B-site cations because of settling of Zr<sup>4+</sup> ions randomly in the B-site [35]. Since the random settling of Zr<sup>4+</sup> ions in B-site accompanying with Yb<sup>3+</sup> and Nb<sup>5+</sup> ions, which have higher ionic radii differences, results in existing nonhomogenous structural disorder which triggers DPT [35]. Similarly, addition of Pb(Fe<sub>1/2</sub>Nb<sub>1/2</sub>)O<sub>3</sub> (PFN) to PYbN system resulted in broadened phase transition and decreased  $K_{\max}$  [36].

The variation of remnant polarization ( $P_r$ ) and coercive field ( $E_c$ ) as a function of sintering temperature is compared in Fig. 6. Parallel to the dielectric properties, samples reached to their respective maximum values when they had higher density and perovskite ratio. Samples sintered at around 1000 °C for 4 h, for example, have  $P_r$  values of 23  $\mu\text{C}/\text{cm}^2$ , 32  $\mu\text{C}/\text{cm}^2$ , 34  $\mu\text{C}/\text{cm}^2$  and 36  $\mu\text{C}/\text{cm}^2$  and  $E_c$  values of 21 kV/cm, 17 kV/cm, 11 kV/cm and 10 kV/cm for the R-25, R-50, R-75T and R-75R ceramics, respectively. In addition, the R-75R and R-75T samples show almost constant  $P_r$ - $E_c$  values throughout the

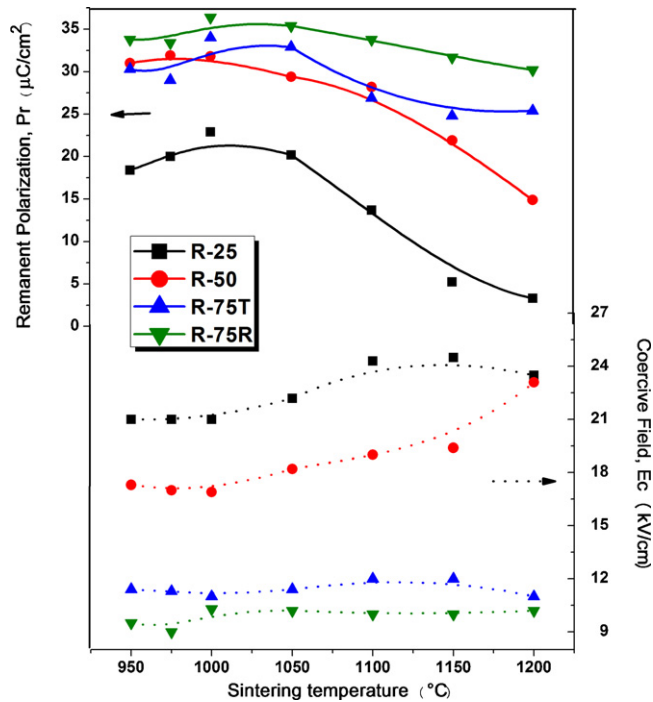


Fig. 6. The variation of  $P_r$  and  $E_c$  for the PMN-PYbN-PT based ceramics as a function of sintering temperature.

studied sintering regime due to their high densities coupled with full perovskite phase. The  $P_r$ - $E_c$  values dramatically changed for the R-25 and R-50 samples particularly when sintered at  $>1000$  °C due to the presence of pyrochlore phase (see Table 2). In fact, about 35% pyrochlore phase for the R-25 ceramics sintered at 1200 °C for 4 h dropped its  $P_r$  down to  $3.3 \mu\text{C}/\text{cm}^2$ . A comparison of polarization-electric field (P-E) hysteresis loops of the R-25, R-50, R-75T and R-75R ceramics sintered at 1000 °C for 4 h and PMNT32.5 ceramic sintered at 1200 °C for 6 h are shown in Fig. 7. In fact, the amount of PYbNT substantially changed the shape of the hysteresis loops.

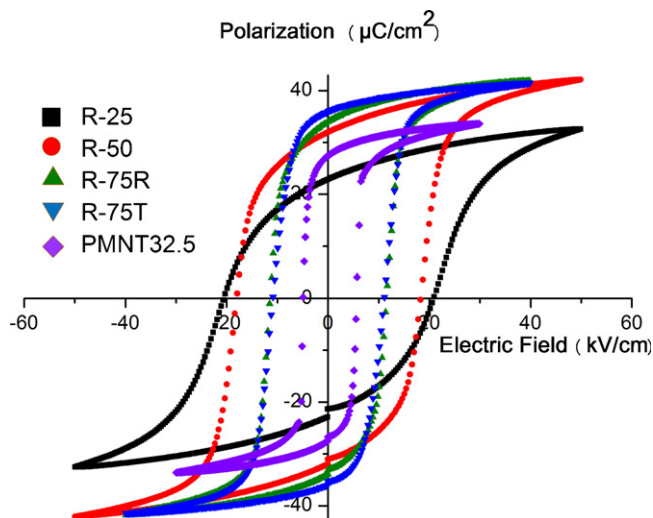


Fig. 7. P-E loops of the PMN-PYbN-PT ceramics sintered at 1000 °C for 4 h and PMNT32.5 sintered at 1200 °C for 6 h.

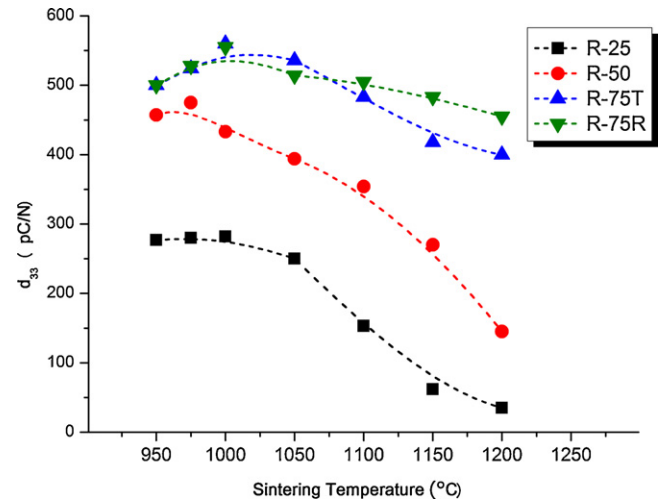


Fig. 8. Piezoelectric charge coefficients ( $d_{33}$ ) of the PMN-PYbN-PT based ceramics as a function of sintering temperature.

The addition of PYbNT into PMNT resulted in well-saturated hysteresis loops with higher  $P_r$  and  $E_c$  than PMNT32.5, except for the R-25 sample [20,26,28,37]. The higher  $P_r$  and  $E_c$  in the R-75R and R-75T samples can be attributed to the incorporation of PYbNT to PMNT because PYbNT possesses  $P_r = 36 \mu\text{C}/\text{cm}^2$  and  $E_c = 22 \text{ kV}/\text{cm}$  [20], as compared with  $P_r = 26.2 \mu\text{C}/\text{cm}^2$  and  $E_c = 4.1 \text{ kV}/\text{cm}$  for PMNT32 [17]. Rhombohedral-rich R-75R ceramics have slightly higher  $P_r$  and lower  $E_c$  than tetragonal-rich R-75T because of the larger number of polarization directions available. Relatively lower  $P_r$  value for the R-50 samples (as compared with the R-75 samples) may be attributed to its relatively higher  $E_c$  value, which is related with the domain switching. As  $E_c$  increases, it becomes difficult to align the domains with the electric field. Since the  $E_c$  of ternary ceramics are 2–4 times higher than the PMNT based ceramics, easy depoling of the PMN-PYbN-PT based ternary compositions under stresses can be prevented.

Fig. 8 depicts piezoelectric charge coefficients ( $d_{33}$ ) of ternary compositions as a function of sintering temperature. Parallel to the dependence of room temperature dielectric constant (Fig. 3) and remnant polarization (Fig. 6) on sintering temperature, maximum  $d_{33}$  values were also observed for ceramics sintered near 1000 °C. The higher piezoelectric  $d_{33}$  values can be attributed in part to the higher  $K$  and  $P_r$  values [20] because the piezoelectric coefficient for a ferroelectric ceramic has been defined as;

$$d_{33} \sim 2Q\varepsilon_0 K P_r \quad (1)$$

where  $Q$  is the electrostrictive coefficient,  $\varepsilon_0$  is the permittivity of free space,  $K$  is the dielectric constant and  $P_r$  is the remnant polarization [18]. The R-75T and R-75R samples sintered at 1000 °C for 4 h have the highest  $d_{33} = 560 \text{ pC}/\text{N}$ , which is comparable to the  $d_{33} = 590 \text{ pC}/\text{N}$  for PMNT32 [38]. Note that PYbNT has a  $d_{33} = 508 \text{ pC}/\text{N}$  [20]. The  $d_{33}$  values of particularly R-25 and R-50 ceramics sintered at  $>1000$  °C decrease sharply due to lower density and increased amount of pyrochlore phase (see in Table 2).

These results show in brief that the incorporation of PYbNT into PMNT induces densification at much lower sintering temperatures (e.g.,  $\leq 1000^\circ\text{C}$ ), does not deteriorate the dielectric and piezoelectric properties, and increases the  $T_c$ . The increase in the  $T_c$  is particularly desired for more stable device applications at higher temperatures.

#### 4. Conclusions

New ternary compositions in the  $\text{Pb}(\text{Mg}_{1/3}\text{Nb}_{2/3})\text{O}_3$ – $\text{Pb}(\text{Yb}_{1/2}\text{Nb}_{1/2})\text{O}_3$ – $\text{PbTiO}_3$  (PMN–PYbN–PT) system were prepared using  $0.5\text{Pb}(\text{Yb}_{1/2}\text{Nb}_{1/2})\text{O}_3$ – $0.5\text{PbTiO}_3$  (PYbNT) and  $(1-x)\text{Pb}(\text{Mg}_{1/3}\text{Nb}_{2/3})\text{O}_3$ – $x\text{PbTiO}_3$  ( $x = 0.26$ ; PMNT26 or  $x = 0.325$ ; PMNT32.5) powders synthesized via the columbite method. Dense ( $\geq 96\%$  of theoretical density) ceramics with PMN/PYbN mole ratios of 25/75 (R-25), 50/50 (R-50) and 75/25 (R-75T and R-75R) were fabricated by reactive sintering at around  $1000^\circ\text{C}$  for 4 h. Therefore, incorporation of PYbNT to PMNT successfully decreased sintering temperature of PMNT from  $1200^\circ\text{C}$ – $1250^\circ\text{C}$  to around  $1000^\circ\text{C}$ . It was found in general that as weight loss increased with increasing sintering temperature, both perovskite ratio and densification decreased. Variation of perovskite stability as a function of PMN/PYbN mole ratio was found to be related to variation of tolerance factor in that increasing PYbN amount decreased the tolerance factor by introducing more  $\text{Yb}^{3+}$  ions to the B-site in the ternary compositions.

Samples with higher density and perovskite ratio together with lower weight loss possessed higher dielectric and piezoelectric values in each composition. The remanent polarization ( $P_r$ ) values of  $23\text{ }\mu\text{C}/\text{cm}^2$ ,  $32\text{ }\mu\text{C}/\text{cm}^2$ ,  $34\text{ }\mu\text{C}/\text{cm}^2$ ,  $36\text{ }\mu\text{C}/\text{cm}^2$  and coercive field ( $E_c$ ) values of  $21\text{ kV}/\text{cm}$ ,  $17\text{ kV}/\text{cm}$ ,  $11\text{ kV}/\text{cm}$ ,  $10\text{ kV}/\text{cm}$  were measured for the R-25, R-50, R-75T, R-75R ceramics sintered at  $1000^\circ\text{C}$  for 4 h, respectively. Similarly, the R-75T and R-75R samples sintered at  $1000^\circ\text{C}$  had the highest piezoelectric charge coefficient ( $d_{33}$ ) =  $560\text{ pC}/\text{N}$  because higher  $d_{33}$  can be attributed in part to the higher room temperature dielectric constant and  $P_r$  values.

Sharp phase transition of PMNT as a function of temperature became broader or more diffuse with increasing PYbNT content. In addition, dielectric loss behavior indicated that depolarization temperature ( $T_d$ ) was different from the Curie temperature ( $T_c$ ). The difference between  $T_c$  and  $T_d$  were calculated to be  $3^\circ\text{C}$ ,  $2^\circ\text{C}$ ,  $8^\circ\text{C}$  and  $24^\circ\text{C}$  for the PMNT32.5, R-75T, R-50 and R-75R ceramics, respectively. The  $T_c$  values were  $183^\circ\text{C}$ ,  $220^\circ\text{C}$ ,  $242^\circ\text{C}$ ,  $282^\circ\text{C}$  and  $336^\circ\text{C}$  (at  $1\text{ kHz}$ ) for PMNT32.5, R-75T, R-75R, R-50 and R-25, respectively. Higher  $T_c$  induced by incorporation of PYbNT to PMNT can be attributed to the higher  $T_c$  of the PYbNT ( $\sim 371^\circ\text{C}$ ). Therefore, these ternary compositions can be tailored for various high temperature applications due to relatively higher  $T_c$  with enhanced piezoelectric and dielectric properties as compared to PMNT.

#### References

- [1] L.E. Cross, Relaxor Ferroelectrics, *Ferroelectrics* 76 (1987) 241–267.
- [2] S.T. Chung, K. Nagata, H. Igarashi, Piezoelectric and Dielectric Properties of PNN–PZN–PZ–PT System Ceramics, *Ferroelectrics* 94 (1989) 243–247.
- [3] Y.-H. Chen, K. Uchino, D. Viehland, Substituent Effects in  $0.65\text{Pb}(\text{Mg}_{1/3}\text{Nb}_{2/3})\text{O}_3$ – $0.35\text{PbTiO}_3$  Piezoelectric Ceramics, *J. Electroceram.* 6 (1) (2001) 13–19.
- [4] O. Furukawa, M. Harata, Y. Yamashita, K. Inagaki, S. Mukaeda, A lead. Perovskite Y5 V Dielectric for Multilayer Ceramic Capacitor, *Jpn. J. Appl. Phys.* 26 (Suppl. 2) (1987) 34–37.
- [5] G.A. Smolenskii, A.I. Agranovskaya, Dielectric Polarization of a Number of Complex Compounds, *Sov. Phys. Solid State* 1 (1959) 1429–1437.
- [6] S.E. Park, T.R. Shrout, Ultrahigh Strain and Piezoelectric Behavior in Relaxor Based Ferroelectric Single Crystals, *J. Appl. Phys.* 82 (1997) 1804–1811.
- [7] S.W. Choi, T.R. Shrout, S.J. Jang, A.S. Bhalla, Dielectric and Pyroelectric Properties in the  $\text{Pb}(\text{Mg}_{1/3}\text{Nb}_{2/3})\text{O}_3$ – $\text{PbTiO}_3$  Systems, *Ferroelectrics* 100 (1989) 29–34.
- [8] T.R. Shrout, J. Fielding Jr., Relaxor Ferroelectric Materials, *Proceedings of IEEE 1990 Ultrasonics Symposium* (1990) 711–720.
- [9] G.H. Haertling, Ferroelectric Ceramics: History and Technology, *J. Am. Ceram. Soc.* 82 (1999) 797–818.
- [10] V.A. Bokov, I.E. Myl'nikova, Piezoelectric Properties of New Compound Single Crystals with Perovskite Structure, *Fiz. Tverd. Tela* 2 (1960) 2728–2732.
- [11] Z. Surowiak, M.F. Kupriyanov, A.E. Panich, R. Skulski, The Properties of the Non-stoichiometric Ceramics  $(1-x)\text{Pb}(\text{Mg}_{1/3}\text{Nb}_{2/3})\text{O}_3$ – $(x)\text{PbTiO}_3$ , *J. Eur. Ceram. Soc.* 21 (2001) 2783–2786.
- [12] K.R. Han, J.W. Jeong, C.-S. Kim, Y.-S. Kwon, Low-temperature Fabrication of  $0.65\text{ PMN}$ – $0.35\text{ PT}$  by a Mixed Oxide Method, *Mater. Letters* 60 (29–30) (2006) 3596–3600.
- [13] S. Kwon, E.M. Sabolsky, G.L. Messing, Low-temperature Reactive Sintering of  $0.65\text{ PMN}$ – $0.35\text{ PT}$ , *J. Am. Cer. Soc.* 84 (3) (2001) 648–650.
- [14] M.N. Rahaman, L.C. De Jonghe, Reaction Sintering of Zinc Ferrite During Constant Rates of Heating, *J. Am. Ceram. Soc.* 76 (7) (1993) 1739–1744.
- [15] P. Kumar, S. Sharma, O.P. Thakur, C. Prakash, T.C. Goel, Dielectric, Piezoelectric and Pyroelectric Properties of PMN–PT (68:32) System, *Ceram. Int.* 30 (2004) 585–589.
- [16] J. Kelly, M. Leonard, C. Tantigate, A. Safari, Effect of Composition on the Electromechanical Properties of  $(1-x)\text{Pb}(\text{Mg}_{1/3}\text{Nb}_{2/3})\text{O}_3$ – $x\text{PbTiO}_3$  Ceramics, *J. Am. Ceram. Soc.* 82 (4) (1999) 797–818.
- [17] L. Cao, X. Yao, Z. Xu, Y. Feng, Research on Dielectric and Piezoelectric Properties of Ta-doped  $0.68\text{Pb}(\text{Mg}_{1/3}\text{Nb}_{2/3})\text{O}_3$ – $0.32\text{PbTiO}_3$  Ceramics, *Ceram. Int.* 30 (2004) 1373–1376.
- [18] S.E. Park, T.R. Shrout, Characteristics of Relaxor-based Piezoelectric Single Crystals for Ultrasonic Transducers, *IEEE Trans. Ferroelectr. Freq. Control* 44 (5) (1997) 1140–1147.
- [19] E. Akça, H. Yilmaz, C. Duran, Processing and Electrical Properties in Lead-Based  $(\text{Pb}(\text{Mg}_{1/3}\text{Nb}_{2/3})\text{O}_3, \text{Pb}(\text{Yb}_{1/2}\text{Nb}_{1/2})\text{O}_3, \text{PbTiO}_3)$  Systems, *J. Am. Cer. Soc.* 93 (1) (2010) 28–31.
- [20] C. Duran, S. Troler-McKinstry, G.L. Messing, Processing and Electrical Properties of  $0.5\text{Pb}(\text{Yb}_{1/2}\text{Nb}_{1/2})\text{O}_3$ – $0.5\text{PbTiO}_3$  Ceramics, *J. Electroceram.* 10 (2003) 47–55.
- [21] S.L. Swartz, T.R. Shourt, Fabrication of Perovskite Lead Magnesium Niobate, *Mater. Res. Bull.* 17 (10) (1982) 1245–1250.
- [22] A. Gultekin, H. Yilmaz, Processing and Electrical Properties of  $(1-x)[(1-y)(\text{Pb}(\text{Mg}_{1/3}\text{Nb}_{2/3})\text{O}_3) - y(\text{Pb}(\text{Yb}_{1/2}\text{Nb}_{1/2})\text{O}_3)] - x\text{PbTiO}_3$  Ceramics, *Mater. Lett.* 63 (2009) 584–586.
- [23] T.R. Shrout, A. Halliyal, Preparation of Lead-Based Ferroelectric Relaxors for Capacitors, *Am. Ceram. Soc. Bull.* 66 (4) (1987) 704–711.
- [24] T. Taniguchi, Y. Yoshikawa, Preparation of Perovskite  $\text{Pb}(\text{B}_{0.5}\text{Nb}_{0.5})\text{O}_3$  (B = Rare-Earth Elements), *J. Electroceramics* 13 (2004) 373–377.
- [25] R.D. Shannon, Revised Effective Ionic Radii and Systematic Studies of Interatomic Distances in Halides and Chalcogenides, *Acta Cryst. A* 32 (1976) 751–767.
- [26] H.-C. Wang, W.A. Schulze, The Role of Excess Magnesium Oxide or Lead Oxide in Determining the Microstructure and Properties of Lead Magnesium Niobate, *J. Am. Ceram. Soc.* 73 (4) (1990) 825–832.

- [27] M. Villegas, A.C. Caballero, M. Kosec, C. Moure, P. Duran, J.F. Fernandez, Effects of PbO Excess in  $\text{Pb}(\text{Mg}_{1/3}\text{Nb}_{2/3})\text{O}_3$ – $\text{PbTiO}_3$  Ceramics: Part I. Sintering and Dielectric Properties, *J. Mater. Res.* 14 (1999) 891–897.
- [28] S.M. Gupta, A.R. Kulkarni, Role of Excess PbO on the Microstructure and Dielectric Properties of Lead Magnesium Niobate, *J. Mater. Res.* 10 (4) (1995) 953–961.
- [29] H.Q. Fan, H.E. Kim, Effect of Lead Content on the Structure and Electrical Properties of  $\text{Pb}((\text{Zn}_{1/3}\text{Nb}_{2/3})(0.5)(\text{Zr}_{0.47}\text{Ti}_{0.53})(0.5))\text{O}_3$  ceramics, *J. Am. Ceram. Soc.* 84 (3) (2001) 636–638.
- [30] M. Antonova, L. Shebanovs, M. Livinsh, J.Y. Yamashita, A. Sternberg, I. Shorubalko, A. Spule, Structure and Properties of Hot-pressed  $\text{Pb}(\text{Lu}_{1/2}\text{Nb}_{1/2})\text{O}_3$ – $\text{PbTiO}_3$  Binary System Ceramics, *J. Electroceramics* 4 (1) (2000) 179–187.
- [31] CRC Handbook of Chemistry and Physics, 66th edn. CRC Press, Boca Raton, FL, E53, (1985/86).
- [32] H.M. Jang, K.-M. Lee, Dielectric and Piezoelectric Properties of the Thermally Annealed  $\text{Pb}(\text{Zn,Mg})_{(1/3)}\text{Nb}_{2/3}\text{O}_3$ – $\text{PbTiO}_3$  System Across The Rhombohedral Tetragonal Morphotropic Phase, *J. Mater. Res.* 10 (12) (1995) 3185–3193.
- [33] K. Uchino, *Ferroelectric Devices*, Marcel Dekker, Inc., 2000, pp. 108–118, ISBN:0-8247-8133-3.
- [34] M. Yokosuka, Ferroelectricity of Solid Solution  $\text{Pb}[(\text{Yb}_{1/2}\text{Nb}_{1/2})_{1/3}\text{Zr}_{2/3}]\text{O}_3$ , *Jpn. J. Appl. Phys.* 33 (8A, Part 2) (1994) L1100.
- [35] K.V. Im, J.-H. Kim, W.K. Choo, A Study of the Dielectric Properties and Diffuse Phase Transition of the  $(1-x)\text{Pb}(\text{Yb}_{1/2}\text{Nb}_{1/2})\text{O}_3$ – $x\text{PbZrO}_3$  Binary System, *IEEE ISAF* 98 (1998).
- [36] J.-R. Kwon, K.-S. Koh, W.K. Choo, A Crystallographic and Dielectric Studies in  $\text{Pb}(\text{Yb}_{1/2}\text{Nb}_{1/2})\text{O}_3$ – $\text{Pb}(\text{Fe}_{1/2}\text{Nb}_{1/2})\text{O}_3$ , *Ferroelectrics* 127 (1992) 161–166.
- [37] M. Alguero, J. Ricote, P. Ramos, R. Jimenez, J. Carreaud, J.-M. Kiat, B.D. Khil and M. Kosec, Size Effects on the Macroscopic Properties of the Relaxor Ferroelectric  $\text{Pb}(\text{Mg}_{1/3}\text{Nb}_{2/3})\text{O}_3$ – $\text{PbTiO}_3$  Solid Solution, *Handbook of Dielectric, Piezoelectric and Ferroelectric Materials Synthesis, Properties and Applications*, Edited by Z.-G. Ye., CRC Press, (2008), 447–467.
- [38] J. Kelly, M. Leonard, C. Tantigate, A. Safari, Effect of Composition on the Electromechanical Properties of  $(1-x)\text{Pb}(\text{Mg}_{1/3}\text{Nb}_{2/3})\text{O}_3$ – $x\text{PbTiO}_3$  Ceramics, *J. Am. Ceram. Soc.* 80 (4) (1997) 957–964.